



# Anion-controlled networks of intermolecular interactions in the crystal structure of 9-aminoacridinium salts

Artur Sikorski\*, Damian Trzybiński

Faculty of Chemistry, University of Gdańsk, J. Sobieskiego 18, 80-952 Gdańsk, Poland

## ARTICLE INFO

### Article history:

Received 31 August 2010  
Received in revised form 6 November 2010  
Accepted 9 December 2010  
Available online 16 December 2010

This paper is dedicated to Professor Jerzy Białejowski on his 65th birthday

### Keywords:

Crystal structure  
9-Aminoacridine  
Hydrogen bonds  
 $\pi$ - $\pi$  Stacking  
Crystal engineering

## ABSTRACT

A series of salts, with the 9-aminoacridinium cation (9-AA) and aromatic carboxylic acid: benzoate (**1**), *ortho*-phthalate (**2**), and salicylate (**3**) anions have been synthesized and characterized using X-ray diffraction. In the crystal packing, the ions are linked via N–H $\cdots$ O, O–H $\cdots$ O, and C–H $\cdots$ O hydrogen bonds. Analysis of the hydrogen bonds in the crystal lattices of the title compounds shows that the cations and anions form tetramers. The ions in these tetramers are linked via N(amino)–H $\cdots$ O(carboxy) hydrogen bonds forming R<sub>2</sub><sup>2</sup>(8) (**1** and **3**) or R<sub>2</sub><sup>4</sup>(15) (**2**) hydrogen bond ring motifs. The cations interact through  $\pi$ - $\pi$  interactions in the ABBA (**1**), AB (**2**) or ABA (**3**) arrangement to form columns (**1** and **2**) or chains (**3**).

© 2010 Elsevier Ltd. All rights reserved.

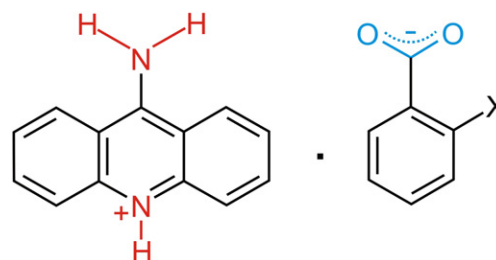
## 1. Introduction

9-Aminoacridine (9-AA) and its derivatives present a very interesting object of research. This group of compounds exhibits a wide spectrum of biological activities: antiamebic, antibacterial, antiprion, antitumor, antiinflammatory, antiimplantation, hyper-tensive, and mutagenic.<sup>1</sup> The potency of acridines as agents is due to their ability to bind DNA through intercalation.<sup>2</sup> 9-AA is also used as a  $\Delta$ pH-probe in a variety of biological systems.<sup>3</sup>

X-ray crystallographic investigations have been carried out on the salts of 9-aminoacridine derivatives with different kind of acids in attempts to understand their specific properties.<sup>4</sup>

In this communication we report the synthesis and X-ray characterization of a series of salts with the 9-aminoacridine cation and the anions of aromatic carboxylic acids—benzoic (**1**), *ortho*-phthalic (**2**), and salicylic (**3**).

9-AA is one of the simplest representatives of the group of organic bases able to interact with biomolecules. The 9-AA cation consists of three conjugated aromatic rings with an extended  $\pi$  system and contains two basic sites situated in the heterocyclic (in the acridine skeleton) and exocyclic (in the amino-group) N atoms (Scheme 1).



**Scheme 1.** Donor–acceptor system in the 9-aminoacridinium–aromatic carboxylic acid anion salts, where X=H (**1**), –COOH (**2**), and –OH (**3**).

With such a structure, this cation can interact with different kinds of anions via strong N–H $\cdots$ X or weak C–H $\cdots$ X, N–H $\cdots$  $\pi$ , C–H $\cdots$  $\pi$  hydrogen bonds, and  $\pi$ -stacking interactions. On the other hand, aromatic carboxylic acid anions have two O atoms that are strong hydrogen bonding acceptors and an aromatic ring, which may interact through a C–H $\cdots$ X hydrogen bond or play a  $\pi$ -electron donor/acceptor role. In this context, an understanding of how these ions aggregate in crystal structures may provide some interesting insight into the influences of different kind anions on the geometry and packing of the 9-AA cation in the crystal lattice.

\* Corresponding author. Tel.: +48 58 523 5425; fax: +48 58 523 54 72; e-mail address: [art@chem.univ.gda.pl](mailto:art@chem.univ.gda.pl) (A. Sikorski).

## 2. Results and discussion

### 2.1. 9-Aminoacridinium benzoate (**1**)

Single-crystal X-ray diffraction measurements show that compound **1** crystallizes in the triclinic  $P\bar{1}$  space group with two 9-AA cations, benzoic acid anions, and water molecules in the asymmetric unit (Fig. S1, Table S1, Supplementary data).

In the packing of the molecules in **1**, the crystal structure is stabilized by N–H···O, O–H···O, and C–H···O hydrogen bonds (Table S2, Supplementary data) and  $\pi$ – $\pi$  interactions (Table S3, Supplementary data). Analysis of the hydrogen bonds in the structure of **1** has shown that the ions form tetramers in the crystal lattice. In these tetramers the ions are inverted via crystallographic inversion center, and both cations A and B and the anions from the asymmetric unit are involved in the formation of the  $R_2^2(8)$  hydrogen bond ring motif (Fig. 1). In this motif, amino groups from the cations and one O-atom of the carboxy-group from the anions participate in the hydrogen bonds. Additionally, the O(carboxy)-atoms engaged in the formation of this motif also take part in weak C(acridine)–H···O (carboxy) hydrogen bonds. The water molecules in the crystal lattice of **1** act as linkers between the tetramers. The tetramers in **1** are connected by N(acridine)–H···O(water) hydrogen bonds, where the O-atoms from the water molecules are acceptors for H-atoms bonded to endocyclic N-atoms from the acridine skeleton. The tetramers of **1** are additionally linked via an O(water)–H···O(carboxy) hydrogen bond, where the O-atoms from the carboxy-groups do not participate in tetramer formation. The water molecules also interact with each other via O–H···O hydrogen bonds (O···O=2.804 Å) (Fig. 1a). Analysis of the  $\pi$ – $\pi$  interactions in **1** shows that the

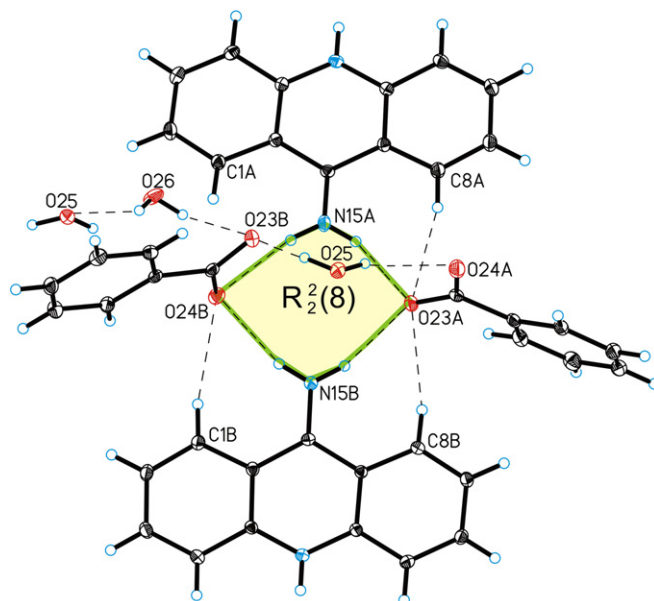


Fig. 1. Network the hydrogen bonds in the structure of **1** ( $R_2^2(8)$  hydrogen bond ring motif is highlighted in yellow).

adjacent 'head to tail' oriented acridine skeletons are linked via  $\pi$ – $\pi$  stacking interactions in the ABBA arrangement to form columns (Fig. 2). All the aromatic rings from the acridine skeletons participate in  $\pi$ – $\pi$  interactions and form a zigzag motif with centroid···centroid

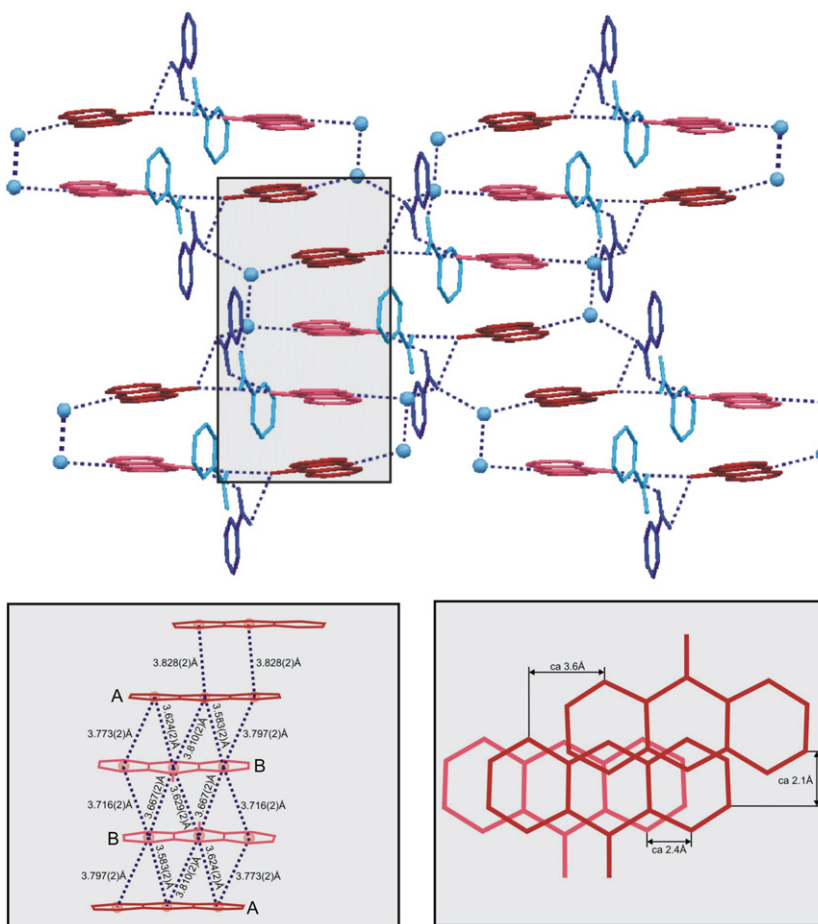


Fig. 2.  $\pi$ – $\pi$  interactions in **1** (the column of acridine skeletons has shown as shadowed rectangle).

distances from 3.583 to 3.810 Å and distance between mean planes of the neighboring acridine skeleton 3.488 Å. In this arrangement, the overlapping mode of neighboring cations shows that they are alternately shifted along the longer axis of the acridine skeleton by a distance of ca. 2.4 Å. The neighboring *ABBA* arrangements are shifted toward each other along the longer axis (by ca. 3.6 Å) and the shorter axis of the acridine skeleton (about ca. 2.1 Å) and linked through two, parallel  $\pi$ – $\pi$  interactions between the A cations (centroid⋯centroid=3.828 Å). Analysis of  $\pi$ – $\pi$  interactions between the aromatic rings in the acid anions in **1** indicates that the shortest centroid⋯centroid distance is equal 4.521 Å. This shows that the  $\pi$ –stacking interactions are absent. In the supramolecular architecture of **1**, there are columns forming separated layers in a *stair-case* motif (Fig. S2, Supplementary data).

## 2.2. 9-Aminoacridinium *ortho*-phthalate (**2**)

Compound **2** form the orthorhombic crystals (*Pbc* space group) with 9-AA cation, *ortho*-phthalate acid anion and water molecule in the asymmetric unit (Fig. S3, Table S1, Supplementary data). The crystal structure of **2** is stabilized by N–H⋯O, O–H⋯O, and C–H⋯O hydrogen bonds (Table S4, Supplementary data) and  $\pi$ – $\pi$  interactions (Table S5, Supplementary data).

Analysis of the hydrogen bonds in the structure of **2** has shown that the ions, which form tetramers are linked via N(amino)–H⋯O (carboxy) hydrogen bonds in the crystal lattice, as well as in **1**. However, in the tetramers of **2**, the ions are inverted via the crystallographic glide plane and forming the  $R_2^4(15)$  hydrogen bond ring motif (Fig. 3). The increase in the number of atoms forming the hydrogen bond ring motif from eight in **1** to fifteen in **2** is a consequence of the structure of the *ortho*-phthalic acid anion when

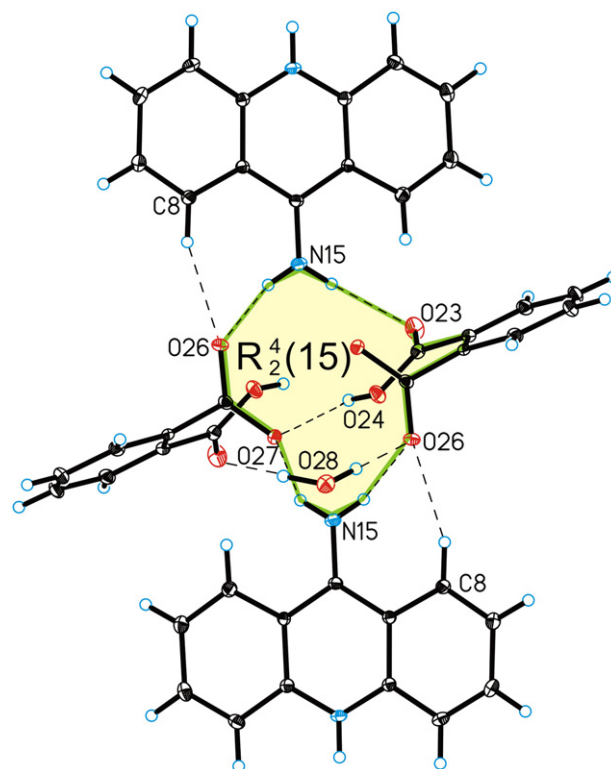


Fig. 3. Network the hydrogen bonds in the structure of **2** ( $R_2^4(15)$  hydrogen bond ring motif is highlighted in yellow).

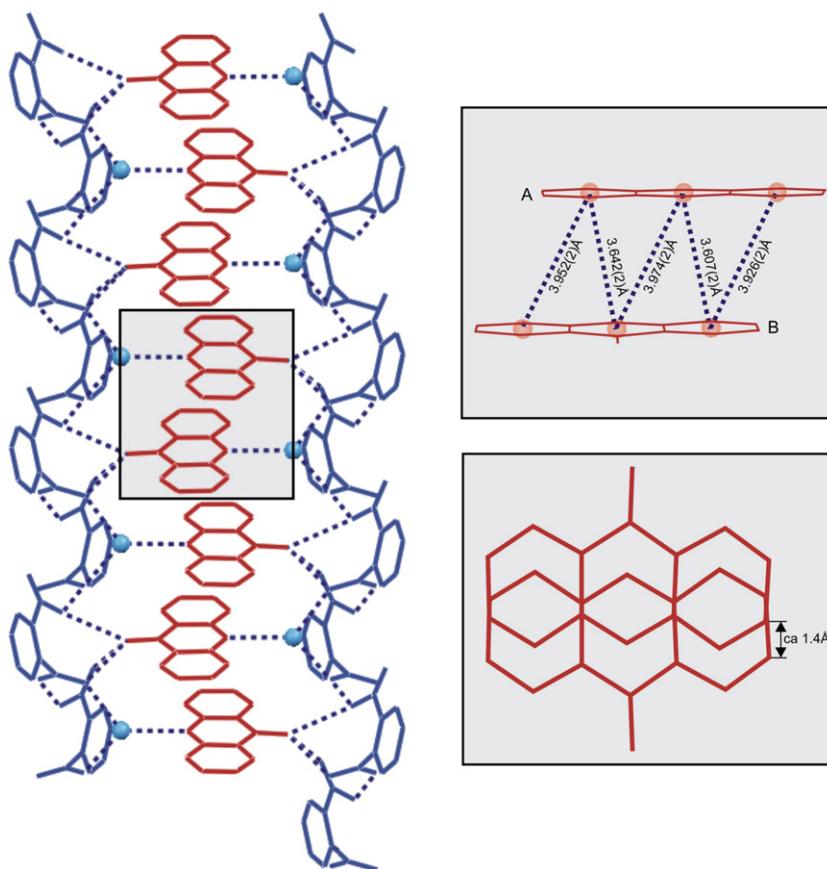


Fig. 4.  $\pi$ – $\pi$  interactions in **2**.

there is one protonated and one deprotonated carboxy group. This means that each deprotonated O-atom from the anion takes part in the formation of this motif. *ortho*-Phthalic acid anions form dimers via O–H···O hydrogen bond between the protonated and deprotonated groups of anions. This hydrogen bond stabilizes the tetramers as well as the C(acridine)–H···O(carboxy) hydrogen bonds. The tetramers in **2** are linked through N(acridine)–H···O(water) and O(water)–H···O(carboxy) hydrogen bond, as in **1**, but there is no O–H···O hydrogen bond between the water molecules (Fig. 4). Analysis of the  $\pi$ – $\pi$  interactions in **2** shows that the ‘head to tail’ oriented neighboring acridine skeletons in **2** interact through  $\pi$ –stacking interactions in an AB arrangement forming columns. In this arrangement, the  $\pi$ – $\pi$  interactions with centroid···centroid distances from 3.607 to 3.974 Å and distance between mean planes of the neighboring acridine skeleton 3.395 Å form a zigzag motif, as in **1**. In the overlapping mode of the neighboring acridine skeletons, adjacent cations are alternately shifted along the shortest axis of the acridine skeletons for a distance of ca. 1.4 Å. Analysis of  $\pi$ – $\pi$  interactions between the aromatic rings in the acid anions in **2** show that the shortest centroid···centroid distance is 4.034 Å. This indicates that the  $\pi$ –stacking interactions between benzene rings from the acid anions are very weak. In the supramolecular architecture of **2**, there are columns that form separate monolayers in a zigzag motif (Fig. S4, Supplementary data).

### 2.3. 9-Aminoacridinium salicylate (**3**)

Compound **3** crystallizes in the triclinic *P*–1 space group. The asymmetric unit of **3** consists of two 9-AA cations and two salicylic acid anions the water molecules are unobserved (Fig. S5, Table S1, Supplementary data). The crystal structure of **3** is stabilized by N–H···O, O–H···O, and C–H···O hydrogen bonds (Table S6,

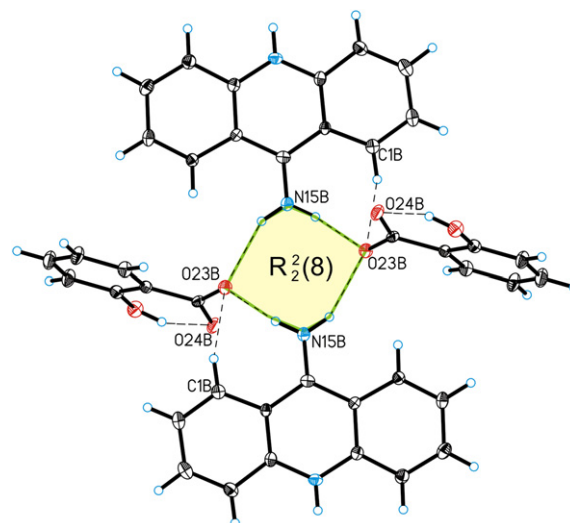


Fig. 5. Network the hydrogen bonds in the structure of **3** ( $R_2^2(8)$  hydrogen bond ring motif is highlighted in yellow).

Supplementary data) and  $\pi$ – $\pi$  interactions (Table S7, Supplementary data).

Analysis of the hydrogen bonds in **3** shows that the ions form tetramers in the crystal lattices and in these tetramers the neighboring cations and anions are linked via N(amino)–H···O(carboxy) hydrogen bonds, as well as in **1** and **2**. In the structure of **3**, the ions in the tetramers, inverted around a center of symmetry, form the  $R_2^2(8)$  hydrogen bond ring motif, as in **1** (Fig. 5). However, in contrast to **1**, there are two kinds of tetramers forming this motif. The first tetramer is formed only when A cations and anions from the

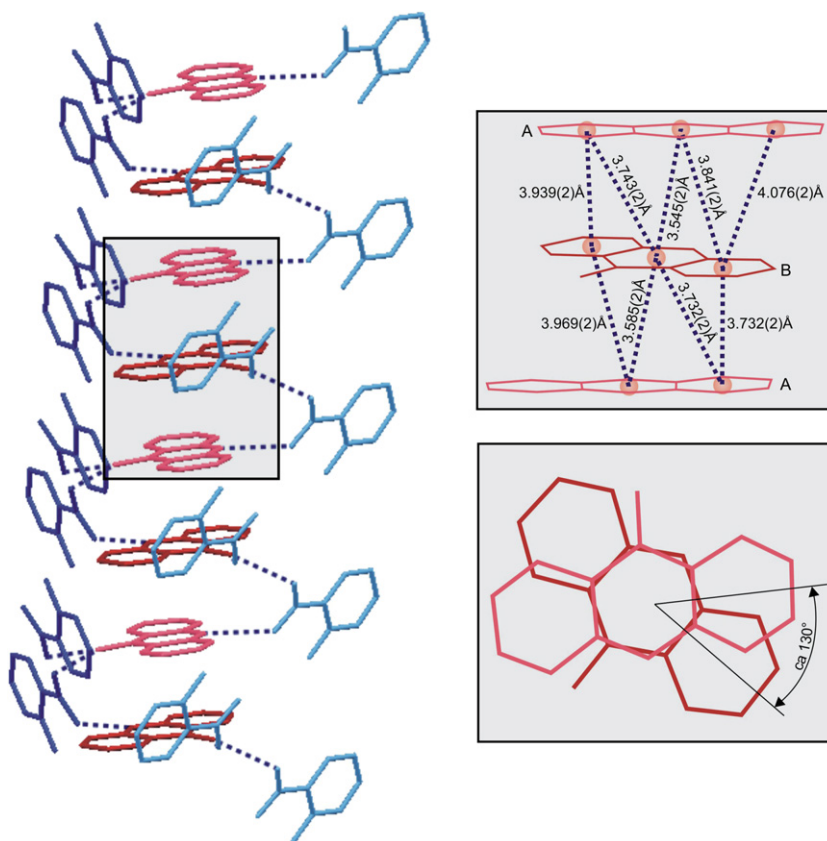


Fig. 6.  $\pi$ – $\pi$  interactions in **3**.

asymmetric unit are present, and the second only when B ions aggregate in the tetramers. In both tetramers, only one O-atom from the carboxy group is engaged in the hydrogen bond ring motif.

This atom is also involved in weak C(acridine)–H···O(carboxy) hydrogen bonds, which stabilize the tetramers. The second O-atom from the carboxy group is involved in an intramolecular O–H···O hydrogen bond, where the hydroxyl groups are donors of H-atoms. Despite the fact that there is no water molecule in the structure of **3**, in contrast to the other compounds, this O-atom is involved in the N(acridine)–H···O(carboxy) hydrogen bonds that link the tetramers. In the crystal lattice of **3**, the neighboring acridine skeletons are linked by  $\pi$ – $\pi$  interactions in the ABA arrangement forming chains (Fig. 6). This is caused by the fact that the adjacent acridine skeletons are not shifted but rotated in-plane with respect to one another by approximately  $130^\circ$ . As a result of this rotation, the  $\pi$ – $\pi$  interactions between the acridine skeletons form a zigzag motif with centroid···centroid distances in the 3.545–4.076 Å range and distance between mean planes of the neighboring acridine skeleton 3.405 Å. In this arrangement, however, only two aromatic rings of cation A are involved in the  $\pi$ -stack interactions between the neighboring B and A cations. Analysis of the centroid···centroid distances in this sequence shows that the distance between one pair of the lateral aromatic rings, equal to 4.325 Å, is too long to be classed as a  $\pi$ – $\pi$  interaction. Analysis of  $\pi$ – $\pi$  interactions between the aromatic rings in the acid anions in **3** show that the shortest centroid···centroid distances is 4.326 Å. This indicates that the  $\pi$ -stacking interactions between benzene ring from the acid anions are absent. In the supramolecular architecture of **2**, there are chains

that form separate monolayers in a zigzag motif (Fig. S6, Supplementary data).

In comparison to the title compounds, in the crystal structure of 9-aminoacridine, which crystallizes as a hemihydrate,<sup>5</sup> the molecules are aggregated in tetramers via N(amino)–H···N(acridine) hydrogen bond, forming the  $R_2^2(8)$  hydrogen bond ring motif, as in **1** and **3** (Fig. 7a). The water molecule connects the tetramers to one another by means of an O(water)–H···N(acridine) hydrogen bond. It is interesting that there are no  $\pi$ – $\pi$  interactions between the acridine skeletons in the structure of the 9-aminoacridine monohydrate. However, the acridine skeletons rotating around the center of symmetry interact through C–H··· $\pi$  interactions. In the crystal packing of the 9-aminoacridine monohydrate we can observe the supramolecular helical tubes, which are not present in the lattices of the title compounds (Fig. 7b).

### 3. Conclusion

To conclude: we report on the structures of a series of 9-aminoacridinium salts with aromatic carboxylic acids. Conformational analysis of the hydrogen bonds in the crystal lattices of the title compounds shows that the cations and anions form tetramers and that the building of anions influences the geometry of the hydrogen bond ring motifs, which are observed in the crystal packing of all compounds. The ions in these tetramers are linked via N(amino)–H···O(carboxy) hydrogen bonds forming  $R_2^2(8)$  (**1** and **3**) or  $R_4^4(15)$  (**2**) hydrogen bond ring motifs. We also observe that the presence of different kinds of anion determines how acridine skeletons interact between themselves in the crystal packing. The 9-AA cations interact only through  $\pi$ – $\pi$  interactions in the ABBA (**1**), AB (**2**) or ABA (**3**) arrangement to form columns (**1** and **2**) or chains (**3**). On the other hand, analysis of  $\pi$ – $\pi$  interactions between the aromatic rings in the acid anions indicates that the shortest centroid···centroid distances are 4.521, 4.034, and 4.326 Å in **1**, **2**, and **3**, respectively. This shows that the  $\pi$ -stacking interactions are either very weak (**2**) or absent altogether (**1** and **3**).

## 4. Experimental

### 4.1. General

The synthesis of compounds **1**, **2**, and **3** is described in Supplementary data. Single crystals of **1–3** were grown by slow evaporation of an ethanol solution.

### 4.2. Crystal structure determination

Good-quality single-crystal specimens of **1**, **2**, and **3** were selected for the X-ray diffraction experiments at  $T=295(2)$  K. They were mounted with epoxy glue at the tip of glass capillaries. Diffraction data were collected on a Oxford Diffraction Gemini R ULTRA Ruby CCD diffractometer with Mo  $K\alpha$  radiation ( $\lambda=0.71073$  Å). In all cases, lattice parameters were obtained by least-squares fit to the optimized setting angles of the collected reflections by means of CrysAlis CCD<sup>6</sup> Data were reduced by using CrysAlis RED software with applying multi-scan absorption corrections (Empirical absorption correction using spherical harmonics, implemented in SCALE3 ABSPACK scaling algorithm). The structural resolution procedure was made using the SHELXS-97 package solving the structures by direct methods and carrying out refinements by full-matrix least-squares on  $F^2$  using SHELXL-97 program.<sup>7</sup> All interactions demonstrated were found by PLATON program.<sup>8</sup>

Crystallographic data for the structures reported in this paper have been deposited with the Cambridge Crystallographic Data Centre as supplementary publication no. CCDC-770732 (**1**), CCDC-770733 (**2**), and CCDC-770734 (**3**). Copies of the data can be obtained

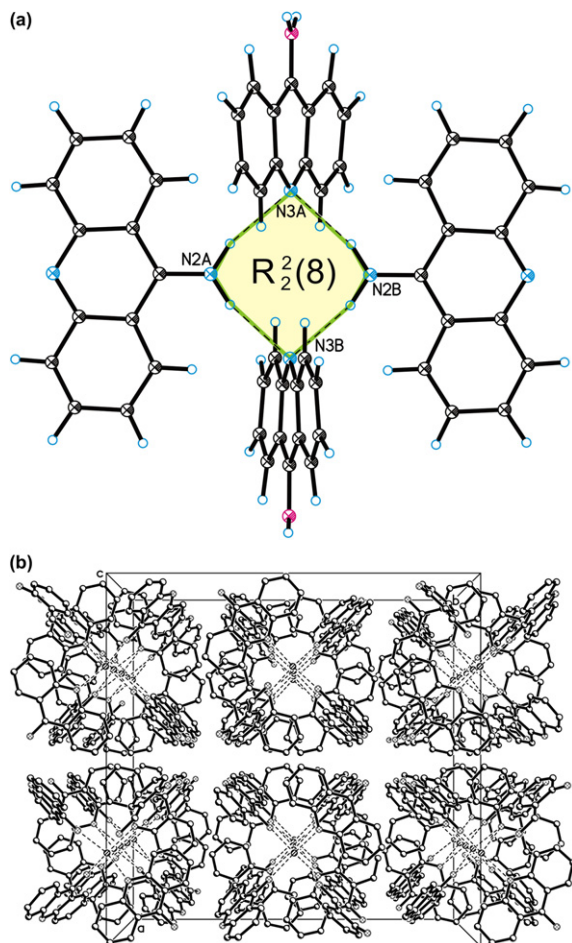


Fig. 7. Network of the intermolecular interactions in the crystal structure of 9-aminoacridine monohydrate: hydrogen bonds (a) and crystal packing (b).

free of charge on application to CCDC, 12 Union Road, Cambridge CB2 1EZ, UK (fax: +44 1223 336 033; e-mail: [deposit@ccdc.cam.ac.uk](mailto:deposit@ccdc.cam.ac.uk)).

### Acknowledgements

This study was financed by the State Funds for Scientific Research (DS/8220-4-0087-10 and BW 8220-5-0466-0). The authors would like to thank J. Zawadzka, N. Targowska and W. Badziąg for their help in the crystallization of title compounds.

### Supplementary data

Electronic supplementary data (ESI) available: experimental details; crystal and structure refinement data for **1**, **2**, and **3**; figures; hydrogen bonds; and  $\pi$ – $\pi$  interactions geometry. For ESI and crystallographic data in CIF or other electronic format are available. Supplementary data associated with this article can be found in online version at [doi:10.1016/j.tet.2010.12.027](https://doi.org/10.1016/j.tet.2010.12.027).

### References and notes

1. Shubber, E. K.; Jacobson-Kram, D.; Williams, J. R. *Cell Biol. Toxicol.* **1986**, *3*, 379–399; Stark, M. M.; Hall, N. C.; Nicholson, R. J.; Soelberg, K. *Oral Surg., Oral Med., Oral Pathol.* **1968**, *26*, 560–562; Nguyen Thi, H. T.; Lee, C.-Y.; Teruya, K.; Ong, W.-Y.; Doh-ura, K.; Go, M.-L. *Bioorg. Med. Chem.* **2008**, *16*, 6737–6746; Belmont, P.; Bosson, J.; Godet, T.; Tiano, M. *Anticancer Agents Med. Chem.* **2007**, *7*, 139–169; Sondhi, S. M.; Singh, N.; Kumar, A.; Lozach, O.; Meijer, L. *Bioorg. Med. Chem.* **2006**, *14*, 3758–3765; Asthana, P.; Rastogi, S.; Ghose, S.; Das, S. R. *Indian J. Chem.* **1991**, *30B*, 893–900; Salamanca, D. A.; Khalil, R. A. *Biochem. Pharmacol.* **2005**, *70*, 1537–1547; Sakore, T. D.; Jain, S. C.; Tsai, C.-C.; Sobell, H. M. *Proc. Natl. Acad. Sci. U.S.A.* **1977**, *74*, 188–192.
2. Martínez, R.; Chacón-García, L. *Curr. Med. Chem.* **2005**, *12*, 127–151.
3. Casadio, R.; Melandri, B. A. *Arch. Biochem. Biophys.* **1985**, *238*, 219–228.
4. Ghose, S.; Chakrabarti, C.; Dattagupta, J. K. *J. Crystallogr. Spectrosc. Res.* **1987**, *17*, 197–201; Ghose, S.; Chakrabarti, C.; Dattagupta, J. K.; Le Page, Y.; Trotter, J. *Acta Crystallogr.* **1988**, *C44*, 1810–1813; Smith, G.; Wermuth, U. D. *Acta Crystallogr.* **2008**, *C64*, o428–o430; Smith, G.; Wermuth, U. D.; Sagatys, D. S. *Acta Crystallogr.* **2009**, *C65*, o131–o133.
5. Chaudhuri, S. J. *Chem. Soc., Chem. Commun.* **1983**, 1242–1243.
6. *CrysAlis CCD and CrysAlis RED*; Oxford Diffraction: Yarnton, England, 2008.
7. Sheldrick, G. M. *Acta Crystallogr.* **2008**, *A64*, 112–122.
8. Spek, A. L. *Acta Crystallogr.* **2009**, *D65*, 148–155.